



Trade Science Inc.

Environmental Science

An Indian Journal

Current Research Paper

ESAIJ, 7(4), 2012 [130-137]

Study of retention of silver ions onto activated carbon prepared from almond shell: Approach for the treatment of liquid effluent from radiology

Abdessalem Omri*, Haithem Bel Haj Ltaief, Mourad Benzina

Laboratory of Water-Energy-Environment (LR3E), Code: AD-10-02, National School of Engineers of Sfax, University of Sfax, BP W, 3038 Sfax, (TUNISIA)

E-mail: omriabdeslem@yahoo.fr

Received: 17th January, 2012 ; Accepted: 10th February, 2012

ABSTRACT

This work reports the retention of silver ions from synthetic solution of silver nitrate regarded as a model of radiological effluent by prepared activated carbon. The effect of initial concentration of silver (I) ions, contact time and temperature on the retention process was studied in a batch process mode. The adsorption was relatively fast and equilibrium was established about 60 min. Equilibrium data were analyzed by the Langmuir and Freundlich isotherm model. The adsorption kinetics was found to be best represented by the pseudo-second-order kinetic model. Thermodynamic study showed that the adsorption was a spontaneous and endothermic process. Characterization of the activated carbon obtained from almond shell (ASC) was performed by using scanning electron microscopy (SEM), Fourier transform infrared spectroscopy (FTIR) and specific surface.

© 2012 Trade Science Inc. - INDIA

KEYWORDS

Activated carbon;
Silver (I) ions;
Retention;
Kinetics.

INTRODUCTION

Silver is considered of special economic interest compared with other metals. Silver nitrate is the most common soluble salt that is used in porcelain, mirroring, photographic, electroplating, and ink formulation industries^[22]. Most world silver is recovered from scraps such as photographic films, X-ray films and jewellery^[3]. Thus it is necessary to treat the waste aqueous solutions and try to recover them economically. Environmental poisoning due to the emission of waste metals from the mineral processing industry in the last

few decades has been and continues to be of growing concern, also recent developments in environmental quality standards highlight the need for improved wastewater treatment of dilute metal-bearing effluents. A number of adsorbents have been developed and tested for the removal and recovery of silver (I) (e.g., activated carbon^[27,28], cellulose nitrate membrane^[29] and chelating resins^[37]). Many studies have appeared on the development of low-cost activated carbon adsorbents produced from cheaper and readily available materials in the literature^[8]. Activated carbons with their large surface area, microporous character and chemical na-

ture of their surface have made them potential adsorbents for the removal of heavy metals from industrial wastewater. Therefore, in recent years, many researchers have tried to produce activated carbons for removal of various pollutants using renewable and cheaper precursors which were mainly industrial and agricultural byproducts, such as coconut shells^[36], waste apricot^[9], palm shell, molasses^[18], rubber wood sawdust^[24], rice straw^[33], seaweed^[5], sugarcane bagasse pith^[4], oil palm fibre^[31] and mangosteen shell^[35].

This study reports the use of almond shell activated carbon (ASC) produced by pyrolysis and physical activation in the presence of water vapor, as an adsorbent to remove of silver (I) ions from synthetic solution of silver nitrate regarded as a model of radiological effluent. At present, this almond shell material is used principally as a solid fuel and is available in abundance in Sfax, Tunisia. The production of almond shell is estimated to exceed 60,000 t / year.

In this study, the experimental parameters for the adsorption of Ag(I) ions from aqueous solutions under different equilibrium conditions were investigated in a batch study. The equilibrium isotherm data were treated with two adsorption isotherm models, Langmuir and Freundlich. Values of kinetics studies of Ag(I) have been reported. In addition to this, characterization of ASC was studied in terms of surface area, surface morphology and surface chemical.

EXPERIMENTAL PROCEDURE

Materials

Almond shell was collected from from a company "Chaabane" located in Sfax, Tunisia. The starting material was cleaned with water and dried at 110 °C for 48 h. The dried sample was crushed with a blender and sieved to desired mesh size (1–2 mm). The synthetic solution of silver nitrate (Merck, > 99 % purity) was used as a source of Ag(I).

Adsorbent preparation

Activated carbons were prepared from almond shell by carbonization under nitrogen flow and activation under water vapor. Carbonization was carried in a vertical stainless-steel reactor (length 170 mm, interior diameter 22 mm) which was inserted into a cylindrical

electric furnace Nabertherm. Almond shells were placed into the reactor and heated from room temperature to 400 °C at a constant heating rate of 10 °C/min under nitrogen flow, then held at 400 °C for 1 h. The samples were left to cool down after the carbonization. Activation was carried out in the same furnace. The charcoal obtained was then physically activated at 850 °C for 2 h under a nitrogen flow (100 cm³/min) saturated in steam after passing through the water saturator heated at 80 °C. The tenor steam was varied to the range of 0.395 kg H₂O/kg N₂. After activation, the sample was cooled to ambient temperature under N₂ flow rate. The produced activated carbon was then dried at 105 °C overnight, ground and sifted to obtain a powder with a particle size smaller than 45 µm, and finally kept in hermetic bottle for subsequent uses.

Physico-chemical characteristics of the activated carbon

The surface functional groups were analyzed by using a FT-IR spectroscopy (NICOET spectrometer). The FTIR spectra were recorded between 500 and 4000 cm⁻¹. Microstructure of the sample was examined using a scanning electron microscopy (SEM, Philips XL30 microscope). The specific surface (S_{BET}) is determined of the activated carbon is determined by the adsorption of nitrogen by using an apparatus B.E.T of the type "ASAP 2010".

Procedure for retention of silver (I): batch adsorption

The effects of experimental parameters such as, initial metal ion concentration (170–680 mg/l), and temperature (25–35 °C) on the efficiency retention of Ag(I) ions were studied in a batch mode of operation for a specific period of contact time (0–180 min). The Ag(I) solutions were prepared by dissolving silver nitrate in double distilled water. The pH of the solutions was not varied. For kinetic studies, 50 ml of Ag(I) solution of known initial concentration was taken in a 250 ml screw-cap conical flask with a fixed adsorbent dosage (0.1g) and was agitated in a thermostated rotary shaker for a contact time varied in the range (0–180 min). The content was agitated with a constant stirring rate at 200 rpm, because above this value, the agitation has a strong effect on the adsorption process^[26]. At various time in-

Current Research Paper

tervals, the adsorbent was separated from the samples by filtering and the filtrate was analyzed using a ZEENIT Atomic Absorption. The amount of adsorption at equilibrium, q_e (mg/g), and the retention percentage, % retention, were calculated by the following equations:

$$q_e = \frac{(C_0 - C_e) \cdot V}{m} \quad (1)$$

$$\% \text{ retention} = \frac{C_0 - C_e}{C_0} \times 100 \quad (2)$$

Where C_0 and C_e (mg/l) are the liquid-phase concentrations of Ag(I) initially and at equilibrium, respectively. V is the volume of the solution (l) and m is the mass of dry adsorbent used (g).

RESULTS AND DISCUSSION

Characterization of ASC

SEM micrographs and surface area

The BET surface area of the SAC was 893.62 m²/g. The average pore diameter of 3.101 nm indicated that the ASC was in the mesoporous region. The surface area of ASC was much higher than conventional activated carbons that is, wood-based activated carbon (769 m²/g)^[12] and coal-based activated carbon (331 m²/g)^[20].

The SEM micrographs of ASC samples are given in Figure 1. The external surfaces of these prepared activated carbon show presence cavities and are very irregular, indicating that the porosity of the material was produced by attack of the reagent (H₂O) during activation. The increase in the steam tenor supports the

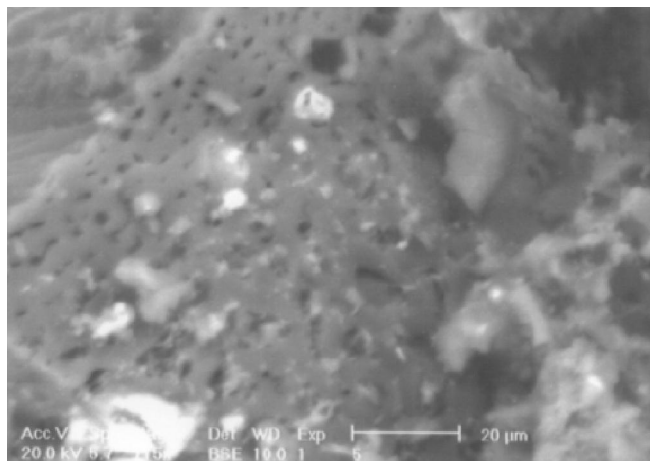


Figure 1 : SEM image of ASC.

following gasification process under high temperature^[30]:



After undergoing carbonization and activation process, the volatile matter content decreased significantly whereas the fixed carbon content increased in ASC. This was due to the pyrolytic effect where most of the organic substances have been degraded and discharged as gas and liquid tars leaving a material with high carbon purity^[2]. Adinata et al.,^[1] found that increasing the carbonization temperature decreased the yield progressively due to released of volatile products as a result of intensifying dehydration and elimination reaction.

IR spectra

The surface chemistry of the samples was evaluated by FTIR. The spectra of the precursor (almond shell) and prepared activated carbons were measured by an FTIR spectrometer within the range of 500–4000 cm⁻¹. The FTIR spectrum of the almond shell is shown in Figure 2. This spectrum is quite similar to that of other lignocellulosic materials such as olive-waste cakes and rockrose^[7, 21]. The FTIR spectrum obtained for the

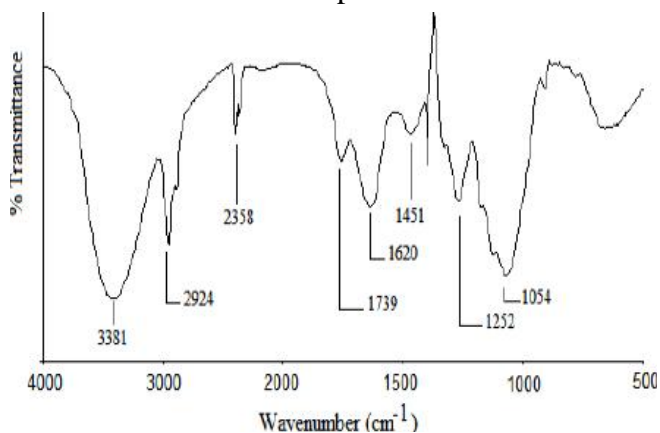


Figure 2 : FTIR spectrum of the almond shell.

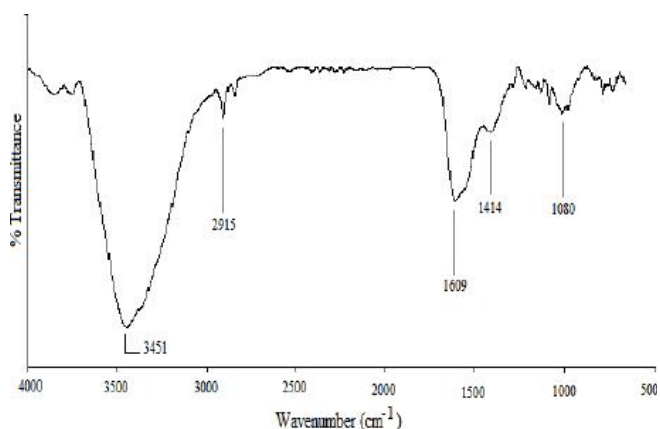


Figure 3 : FTIR spectrum of the ASC.

precursor, the band at about 3381 cm^{-1} was attributed to (O-H) vibrations in hydroxyl groups. The location of hydrogen-bonded OH groups is usually in the range of $3200\text{--}3650\text{ cm}^{-1}$ for alcohols and phenols.

The band observed around 2924 cm^{-1} is attributed to C-H stretching vibration of $-\text{CH}_2$. The band at 2358 cm^{-1} was ascribed to (C=C) vibrations in alkynes groups and methylene groups. The band at 1739 cm^{-1} is ascribed to carbonyl C=O groups. The olefinic (C=C) vibrations cause the emergence of the band at about 1620 cm^{-1} , while the skeletal C=C vibrations in aromatic rings cause another two bands at 1510 and 1425 cm^{-1} . The band at 1252 cm^{-1} may be attributed to esters (e.g. $\text{R-CO-O-R}'$), ethers (e.g. $\text{R-O-R}'$) or phenol groups. The relatively intense band at 1054 cm^{-1} can be assigned to alcohol groups (R-OH)^[7].

Significant changes were observed in the prepared activated carbon FT-IR spectra (Figure 3). Several bands disappeared, which indicates that weak bonds of the initial compounds were broken in the activation process. The bands at 3450 and 1080 cm^{-1} were assigned to O-H bonds and C-OH stretching of phenolic groups, respectively^[13]. The bands located at about 1609 and 1414 cm^{-1} were attributed to carbonyl (e.g. ketone) and carboxylate ion (COO^-) groups, respectively.

Effect of initial silver concentration and contact time

The kinetics of Ag(I) sorption was studied by varying the contact time from 10 min to 180 min using different initial silver concentrations (170, 340, 510 and

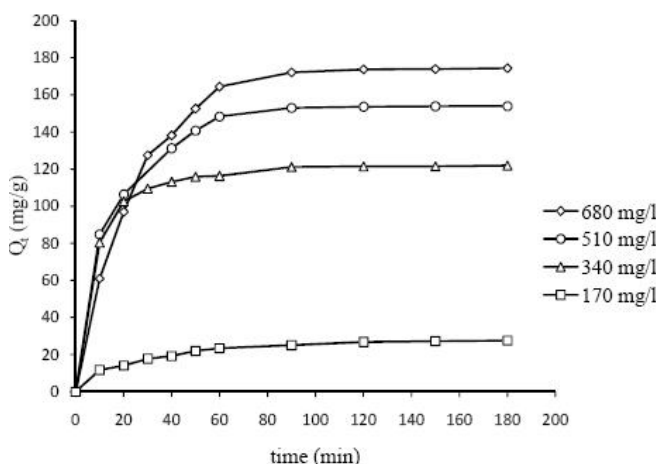


Figure 4 : Effect of initial silver concentration on the retention of Ag(I) by ASC at 298 K.

680 mg/l) and temperatures (298, 308 and 318 K).

The amount of silver adsorbed for different initial concentrations onto ASC is shown in Figure 4. The adsorption of Ag(I) onto ASC increases with time and then attains equilibrium value at a time of about 60 min. The removal of Ag(I) was found to be dependent on the initial concentration, the amount adsorbed increasing with increase in initial concentration. Further, the adsorption is rapid in the early stages and then attains an asymptotic value for larger adsorption time. The same effect was observed on varying the temperature. At low concentrations the ratio of available surface to the initial Ag(I) concentration is larger, so the removal becomes independent of initial concentrations. However, in the case of higher concentrations this ratio is low; the percentage removal then depends upon the initial concentration. On changing the initial concentration from 170 to 680 mg/l, the amount adsorbed increased from 23.4371 to 159.375 mg/g for a time period of 60 min.

Effect of solution temperature

The effect of the temperature on the retention of Ag(I) shows that the percentage increased from 80 to 87.56 % by increasing the temperature from 298 K to 308 K for a time of 60 min (Figure 5). This indicates that the adsorption reaction is endothermic in nature. The variation in the removal may be a result of enhanced escaping tendency of pollutant species at increasing temperatures. The possibility of increased solubility at higher temperatures and hence a lower adsorption can also not be ruled out. Similar trends are also observed by other researchers for aqueous phase adsorption^[11].

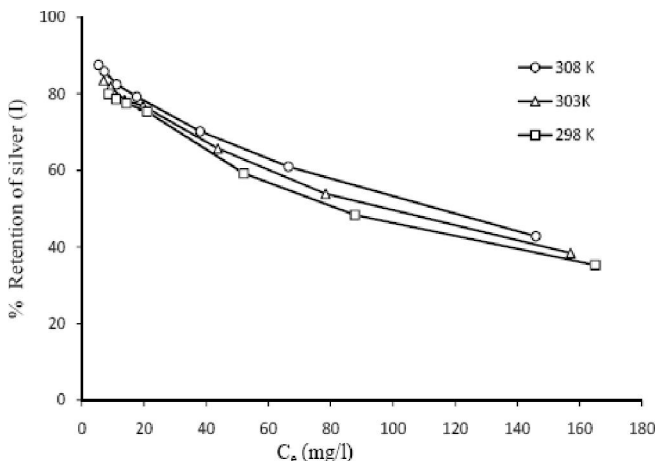


Figure 5 : Effect of temperature on the retention of Ag(I) by ASC at time = 60 min.

Current Research Paper

Adsorption isotherms

Several equilibrium models have been used to describe the equilibrium nature of adsorption. The Langmuir and Freundlich isotherm are the most frequently used models to describe the adsorption data. Langmuir model is based on the assumption that adsorption energy is constant and independent of surface coverage. The maximum adsorption occurs when the surface is covered by a monolayer of adsorbate^[17]. The linear form of Langmuir isotherm equation is given as:

$$\frac{C_e}{q_e} = \frac{1}{Q_m b} + \frac{C_e}{Q_m} \quad (4)$$

Where C_e is the equilibrium concentration of the adsorbate (mg/l), q_e is the amount of adsorbate adsorbed per unit mass of adsorbent (mg/g), b the Langmuir adsorption constant (l/mg), and Q_m is the theoretical maximum adsorption capacity (mg/g).

The essential characteristics of Langmuir equation can be expressed in terms of dimensionless separation factor, R_L , defined as^[34]:

$$R_L = \frac{1}{(1 + bC_0)} \quad (5)$$

Where b is the Langmuir isotherm constant (l/mg) and C_0 is the initial metal concentration (mg/l). The R_L value indicates the type of the isotherm to be either favorable ($0 < R_L < 1$), unfavorable ($R_L > 1$), linear ($R_L = 1$) or irreversible ($R_L = 0$).

Freundlich model is based on sorption on a heterogeneous surface of varied affinities^[15]. The logarithmic form of Freundlich was given as:

$$\log q_e = \log K_F + \left(\frac{1}{n}\right) \log C_e \quad (6)$$

Where K_F and n are Freundlich constants with n as a measure of the deviation of the model from linearity of the adsorption and K_F ($\text{mg/g}(\text{l/mg})^{1/n}$) indicates the adsorption capacity of the adsorbent. In general, $n > 1$ suggests that adsorbate is favorably adsorbed on the adsorbent. The higher the n value the stronger the adsorption intensity.

The plots of $\log q_e$ versus $\log C_e$ and the plots of C_e/q_e versus C_e for the adsorption of Ag(I) onto ASC at at 298, 303 and 308 K according to the linear forms of the Langmuir and Freundlich isotherms are shown in Figures 6 and 7.

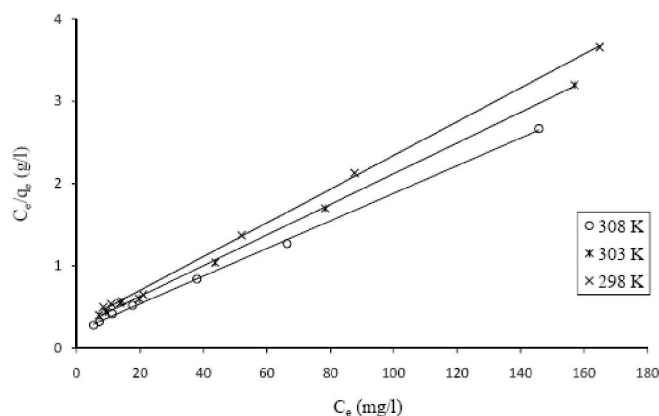


Figure 6 : Langmuir isotherm for adsorption of Ag(I) onto ASC at different temperatures. (temperature =298, 303 and 308 K; t =60 min).

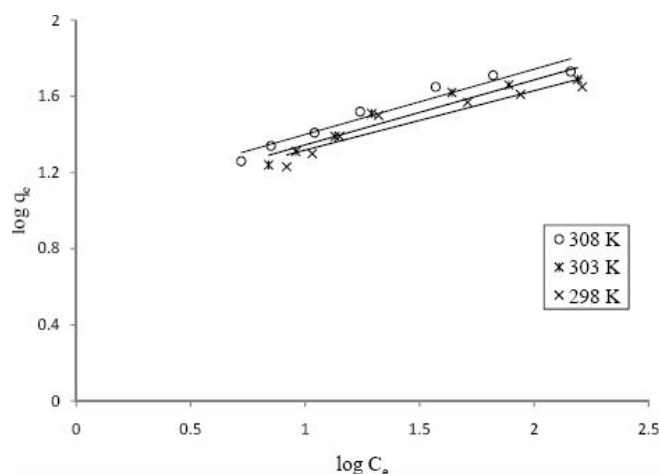


Figure 7 : Freundlich isotherm for adsorption of Ag(I) onto ASC at different temperatures. (temperature =298, 303 and 308 K; t =60 min).

TABLE 1 : Langmuir and Freundlich isotherm parameters for the adsorption of Ag(I) onto ASC at different temperatures.

	Temperatures		
	298 K	303 K	308 K
Langmuir isotherm			
Q_m (mg/g)	48.78	53.76	59.52
b (l/mg)	0.069	0.072	0.082
R_L	0.027	0.026	0.023
R^2	0.998	0.999	0.999
Freundlich isotherm			
K_F (mg/g) (l/mg) ^{1/n}	10.15	10.07	11.40
n	3.215	2.924	2.918
R^2	0.924	0.943	0.902

TABLE 1 summarizes all the constants and correlation coefficient, R^2 values obtained from the two isotherm models applied for adsorption of silver ions on

the ASC. From TABLE 1, the values of n were found to be less than 10 and the values of R_L were in the range of 0.023–0.027 indicating that the adsorption was favorable. The Langmuir isotherms was found to be linear over the whole concentration range studied and the correlation coefficients R^2 , were extremely high compared to the Freundlich isotherms, indicating that the Langmuir isotherm better represented the experimental adsorption data at all solution temperatures. As can be further seen from TABLE 1, the values of Q_m and K_F increased with temperature, indicating that the adsorption process was endothermic in nature.

Adsorption kinetics

In order to analyze the adsorption kinetics of Ag(I) ions onto ASC, two kinetic models; pseudo-first-order and pseudo-second-order kinetic were applied for the experimental data. The pseudo-first-order equation can be expressed as^[16]:

$$\log(q_e - q_t) = \log q_e - \frac{k_1}{2.303} t \tag{7}$$

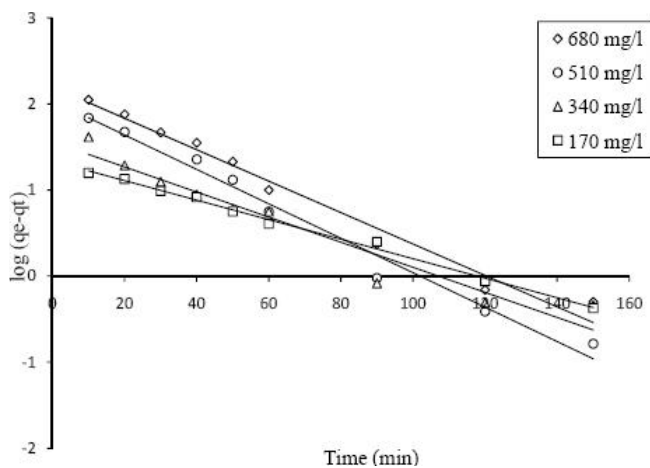


Figure 8 : Pseudo-first-order kinetic plot for the adsorption of Ag(I) onto ASC at 298 K.

TABLE 2 : Pseudo-first order and pseudo-second order kinetic model parameters for the adsorption of Ag(I) onto ASC at 298 K.

[Ag ⁺] (mg/l)	q _e , exp (mg/g)	Pseudo-first-order			Pseudo-second-order		
		q _e , cal (mg/g)	K ₁ (min ⁻¹)	R ²	q _e , cal (mg/g)	K ₂ (g mg ⁻¹ min)	R ²
170	27.125	21.79	0.026	0.994	30.959	0.001	0.998
340	121.425	36.57	0.033	0.938	125	0.002	0.999
510	153.762	109.85	0.045	0.98	161.29	0.0008	0.999
680	173.875	158.7	0.042	0.97	192.307	0.0003	0.995

Where q_e and q_t are the amounts adsorbed at equilibrium and at time t (mg/g), and k_1 is the rate constant of the pseudo-first-order adsorption (min⁻¹). The linear plot of $\log(q_e - q_t)$ versus t gives a slope of k_1 and intercept of $\log q_e$ as shown in Figure 8.

The values of k_1 and R^2 obtained from the plots for adsorption of Ag(I) ions on the adsorbent at 298 K are reported in TABLE 2. It was observed that the R^2 values obtained for the pseudo-first-order model did not show a consistent trend. Besides, the experimental q_e values did not agree with the calculated values obtained from the linear plots. This shows that the adsorption of Ag (I) on the adsorbent does not follow a pseudo first-order kinetic model.

The pseudo-second-order kinetic model can be represented in the following form^[14]:

$$\frac{t}{q_t} = \frac{1}{k_2 q_e^2} + \frac{1}{q_e} t \tag{8}$$

Where k_2 (g/mg min) is the rate constant of second-order adsorption. The linear plot of t/q_t versus t gave $1/q_e$ as the slope and $1/k_2 q_e^2$ as the intercept. Figure 9 shows a good agreement between the experimental and the calculated q_e values. From TABLE 2, all the R^2 values obtained from the pseudo-second-order model were close to unity, indicating that the adsorption of Ag(I) on ASC fitted well into this model.

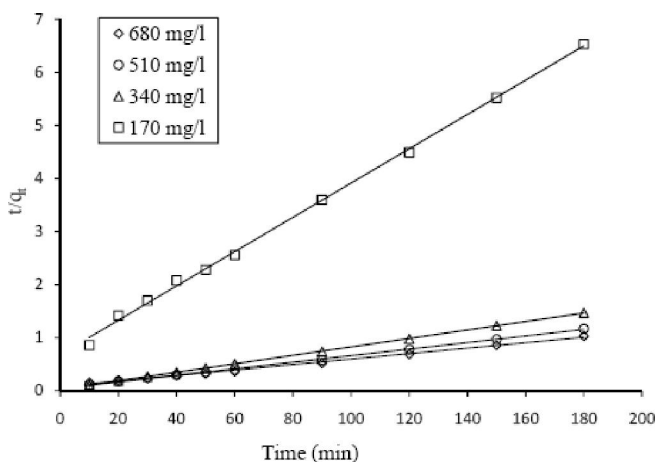


Figure 9 : Pseudo-second-order kinetic plot for the adsorption of Ag(I) onto ASC at 298 K.

Adsorption thermodynamics

The thermodynamic parameters for the present system, including standard free energy (ΔG , kJ/mol), enthalpy (ΔH , kJ/mol) and entropy (ΔS , kJ/mol K), were

Current Research Paper

calculated using following equations Eqs. (9) and (10)^[32]:

$$\Delta G = -RT \ln K \quad (9)$$

$$\Delta G = \Delta H - T\Delta S \quad (10)$$

Where T is the temperature (K), R is universal gas constant (8.314 J/mol K) and K (l/g) is an equilibrium constant obtained by multiplying the Langmuir constant Q_m and b ^[25]. The values of ΔH and ΔS were calculated from the intercept and slope of a plot of ΔG versus T (Figure 10) according to Eq. (10) by linear regression analysis. The calculated thermodynamic parameters were listed in TABLE 3. As shown in TABLE 3, the negative values of ΔG indicated the spontaneous nature of the adsorption process. Positive value of ΔS showed the increasing randomness at the solid–solution interface during the adsorption process^[10,36]. The positive values of ΔH suggested the endothermic nature of the adsorption interaction^[19].

TABLE 3 : Thermodynamic parameters for the retention of Ag(I) onto ASC at different temperatures.

Metal ion	Temperature (K)	ΔG (kJ/mol)	ΔS (kJ/mol K)	ΔH (kJ/mol)
Ag(I)	298	-3.005		
	303	-3.408	0.105	28.446
	308	-4.059		

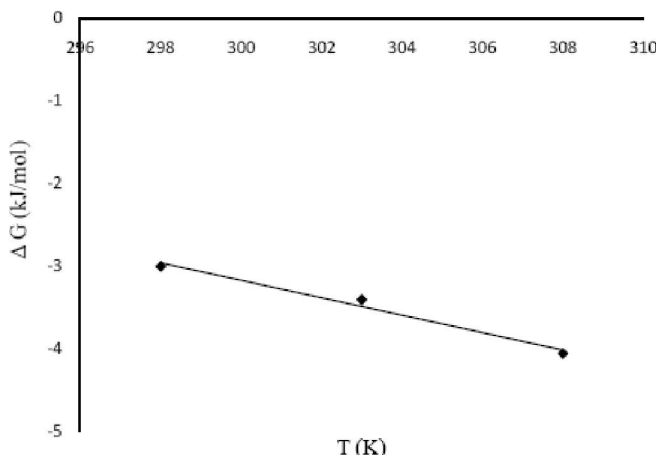


Figure 10 : Plot of ΔG versus T for the estimation of thermodynamic parameters for adsorption of Ag(I) by ASC.

CONCLUSIONS

The present study demonstrates that the prepared activated carbon from almond shell is an effective adsorbent for the retention of Ag(I) from aqueous solutions. Adsorption of silver (I) ions was influenced by

various parameters such as initial metal concentration, contact time and temperature. Efficiency retention increased with decreasing the metal concentration and increasing temperature. The Langmuir and Freundlich adsorption isotherm models were used for the description of the adsorption equilibrium of silver ions onto carbon of almond shell. The data were in good agreement with Langmuir isotherms. It was shown that the adsorption of silver ions best fitted by pseudo-second-order model. From the thermodynamic studies, the adsorption process was endothermic and spontaneous in nature. This activated carbon can be a promising adsorbent for the retention of Ag(I) contained in liquid effluent from radiology.

ACKNOWLEDGEMENTS

The authors thank the Scientific Research Projects Unit of Valorization of the Useful Substances (ENIS) for the support of this work through the project. Also, I thank Mm. Asma BEN ABDELLAH for this linguistic assistance in this manuscript.

REFERENCES

- [1] D.Adinata, W.M.A.Wan Daud, M.K.Aroua; *Bioresour.Technol.*, **98**, 145 (2007).
- [2] M.A.Ahmad, W.M.A.Wan Daud, M.K.Aroua; *J.Oil Palm Res.*, **20**, 453 (2008).
- [3] V.I.E.Ajiwe, I.E.Anyadiegwu; *Sep.Purif.Technol.*, **18**, 89 (2000).
- [4] N.K.Amin; *Desalination*, **223**, 152 (2008).
- [5] R.Aravindhan, R.R.Jonnalagadda, U.N.Balachandran; *J.Taiwan Inst.Chem.Engrs.*, (2011).
- [6] G.M.K.Aroua, N.M.Sulaiman; *Desalination*, **262**, 94 (2010).
- [7] R.Baccar, J.Bouzzid, M.Feki, A.Montiel; *J.Hazard. Mater.*, **162**, 1522 (2009).
- [8] S.E.Bailey, T.J.Olin, R.M.Bricka, D.D.Adrian; *Water Res.*, **33**, 2469 (1999).
- [9] C.A.Başar; *J.Hazard.Mater.*, **B135**, 232 (2006).
- [10] Chakraborty, S.Chakraborty, S.De, S.DasGupta, J.K.Basu; *Chemosphere*, **58**, 1079 (2005).
- [11] S.Chegrouche, A.Mellah, M.Barkat; *Desalination*, **235**, 306 (2009).
- [12] M.A.Diaz-Diez, V.Gomez-Serrano, C.Fernandez Gonzalez; *J.App.Surf.Sci.*, **238**, 309 (2004).

Current Research Paper

- [13] J.L.Figueiredo, M.F.R.Pereira, M.M.A.Freitas, J.J.M.Orfao; *Carbon*, **37**, 1379 (1999).
- [14] A.S.Franca, L.S.Oliveira, M.E.Ferreira; *Desalination*, **249**, 267 (2009).
- [15] H.M.F.Freundlich; *J.Phys.Chem.*, **57**, 385 (1906).
- [16] B.H.Hameed, A.L.Ahmad, K.N.A.Latiff; *Dyes.Pigm.*, **75**, 143 (2007).
- [17] I.Langmuir; *J.Am.Chem.Soc.*, **40**, 1361 (1918).
- [18] K.Legrouri, E.Khouya, M.Ezzine, H.Hannache, R.Denoyel, R.Pallier, R.Naslain; *J.Hazard.Mater.*, **B118**, 259 (2005).
- [19] J.X.Lin, S.L.Zhan, M.H.Fang, X.Q.Qian, H.Yang; *J.Environ.Manage.*, **87**, 193 (2008).
- [20] E.Lorenc-Grabowska, G.Gryglewicz; *J.Dyes.Pig.*, **74**, 34 (2007).
- [21] J.Pastor-Villegas, C.Valenzuela-Calahorro, A.Bernalte-Garcia, V.Gomez-serrano; *Carbon*, **31**, 1061 (1993).
- [22] J.W.Patterson; *Industrial Wastewater Treatment Technology*, 2nd Edition, Butterworth., 405 (1985).
- [23] S.J.T.Pollard, G.F.Fowler, C.J.Sollars, R.Perry; *Sci.Total Environ.*, **116**, 31 (1992).
- [24] B.G.Prakash, K.Kumar, Shivakamy, Lima Rose Miranda, M.Velan; *J.Hazard.Mater.*, **B136**, 922 (2006).
- [25] D.H.K.Reddy, Y.Harinath, K.Seshaiah, A.V.R.Reddy; *Chem.Eng.J.*, **162**, 626 (2010).
- [26] A.D.Souza, P.S.Pina, V.A.Leao, C.A.Silva, P.F.Siqueira; *Hydrometallurgy*, **89**, 72 (2007).
- [27] M.Soylak, L.Elçi, I.Narin, M.Dogan; *Asian J.Chem.*, **13**, 699 (2001).
- [28] M.Soylak, L.Elçi, M.Dogan; *Anal.Lett.*, **33**, 513 (2000).
- [29] M.Soylak, R.S.Çay; *J.Hazard.Mater.*, **146**, 142 (2007).
- [30] I.A.W.Tan, A.L.Ahmad, B.H.Hameed; *J.Hazard.Mater.*, **153**, 709 (2008).
- [31] I.A.W.Tan, B.H.Hameed, A.L.Ahmad; *Chem.Eng. J.*, **127**, 111 (2007).
- [32] L.Wang, J.Zhang, R.Zhao, C.Li, Y.Li, C.L.Zhang; *Desalination*, **254**, 68 (2010).
- [33] S.L.Wang, Y.M.Tzou, Y.H.Lu, G.Sheng; *J.Hazard.Mater.*, **147**, 313 (2007).
- [34] T.W.Weber, R.K.Chakkravorti; *AIChE J.*, **20**, 228 (1974).
- [35] C.Yandan, H.Biao, H.Mingjie, C.Biqiong; *J.Taiwan Inst.Chem.Engrs.*, **42**, 837 (2011).
- [36] K.B.Yang, J.H.Peng, H.Y.Xia, L.B.Zhang, C.Srinivasakannan, S.H.Guo; *J.Taiwan Inst.Chem. Engrs.*, **41**, 367 (2010).
- [37] H.Yirikoglu, M.Gülfen; *Sep.Sci.Technol.*, **43**, 376 (2008).